Toxicology 282 (2011) 94–103

Contents lists available at ScienceDirect

Toxicology

journal homepage: www.elsevier.com/locate/toxicol

An *in vitro* study of vascular endothelial toxicity of CdTe quantum dots

Ming Yan[a], Yun Zhang[a], Kedi Xu[a], Tao Fu[b], Haiyan Qin[b], Xiaoxiang Zheng[a,*]

[a] Department of Biomedical Engineering, Key Laboratory of Biomedical Engineering of Ministry of Education, Zhejiang University, Zheda Road 38, Hangzhou 310027, China
[b] Joint Research Center of Photonics of the Royal Institute of Technology (Sweden) and Zhejiang University, Hangzhou 310058, China

ARTICLE INFO

Article history:
Received 8 October 2010
Received in revised form 21 January 2011
Accepted 22 January 2011
Available online 1 February 2011

Keywords:
Quantum dots
Vascular endothelial cells
Apoptosis
Mitochondrial dysfunction
Reactive oxygen species

ABSTRACT

Quantum dots (QDs), as novel bioimaging and drug delivery agents, are generally introduced into vascular system by injection, and thus directly exposed to vascular endothelial cells (ECs). However, the adverse effects of QDs on ECs are poorly understood. In this study, employing human umbilical vein ECs (HUVECs), we investigated the potential vascular endothelial toxicity of mercaptosuccinic acid (MSA)-capped CdTe QDs *in vitro*. In the experiment, water-soluble and pH stable CdTe QDs were synthesized; and the cell viability assays showed that CdTe QDs (0.1–100 μg/mL) dose-dependently decreased the cell viability of HUVECs, indicating CdTe QDs induced significant endothelial toxicity. The flow cytometric and immunofluorescence results revealed that 10 μg/mL CdTe QDs elicited significant oxidative stress, mitochondrial network fragmentation as well as disruption of mitochondrial membrane potential ($\Delta\psi_m$); whereas ROS scavenger could protect HUVECs from QDs-induced mitochondrial dysfunction. Moreover, upon 24 h exposure to 10 μg/mL CdTe QDs, the apoptotic HUVECs dramatically increased by 402.01%, accompanied with alternative expression of apoptosis proteins, which were upregulation of Bax, downregulation of Bcl-2, release of mitochondrial cytochrome *c* and cleavage of caspase-9/caspase-3. These results suggested that CdTe QDs could not only impair mitochondria but also exert endothelial toxicity through activation of mitochondrial death pathway and induction of endothelial apoptosis. Our results provide strong evidences of the direct toxic effects of QDs on human vascular ECs, and reveal that exposure to QDs is a significant risk for the development of cardiovascular diseases. These results also provide helpful guidance on the future safe use and manipulation of QDs to make them more suitable tools in nanomedicine.

1. Introduction

Semiconductor nanocrystals, which are referred to as quantum dots (QDs), have gain much attention since they were first introduced by Louis Brus and Alexi Ekimov in 1980s (Rossetti et al., 1983; Ekimov et al., 1985). These "artificial atoms" exhibit unique electronic and optical properties such as tunable band gaps, high quantum yields, broad absorption spectra, narrow emission spectra and high resistance to photobleaching. During the past decade, QDs have been developed for a broad range of applications. In the optoelectronic fields, great success has been achieved of using QDs in solar energy conversion, light emitting diodes (LEDs), lasers, and display devices (Huffaker et al., 1998; Likharev, 1999; Coe et al., 2002; Huynh et al., 2002). Meanwhile, in the biomedicine fields, QDs are also successfully utilized as biomedical imaging or traceable drug delivery agents to label biological molecules, cells and even tissues (Resch-Genger et al., 2008), or to follow drug molecules in live organisms (Manabe et al., 2006; Bagalkot et al., 2007). With the spring up of the nascent QD industry, human being is inevitably exposed to these engineered nanomaterials and the studies on the potential toxicity of manufactured QDs become urgent and crucial. Recently, a number of *in vitro* studies have evaluated the toxicity of QDs in different types of cells. For example, Tang et al. tested the neurotoxicity of CdSe QDs in a hippocampal neuronal culture model and a dose-dependent cell death was observed with 24 h continuously exposure to QDs (Tang et al., 2008). Core QDs and QDs with different coatings were also reported to be toxic to primary rat hepatocytes (Shiohara et al., 2004). In addition, the cadmium based QDs were demonstrated to induce dramatic cell loss in pancreatic carcinoma cells (PANC-1), rat pheochromocytoma cells (PC12) and murine microglial cells (N9) (Lovric et al., 2005a; Chang et al., 2009). Although these toxicological studies have shown the toxicity results of cell death for some primary or immortalized cell lines (Derfus et al., 2004; Tang et al., 2008; Su et al., 2009), the understanding of QDs cytotoxicity remains limited.

Lately, QDs were reported to label dermal, adipose, tumor and retinal vasculature (Larson et al., 2003; Cai et al., 2006; Jayagopal et al., 2007). These angiographic techniques provide

* Corresponding author at: Department of Biomedical Engineering, College of Biomedical Engineering & Instrument Science, Zhejiang University, Hangzhou, China. Tel.: +86 571 87953860; fax: +86 571 87951091.
E-mail addresses: zjubme2010@gmail.com, zxx@mail.bme.zju.edu.cn (X. Zheng).

0300-483X/$ – see front matter © 2011 Elsevier Ireland Ltd. All rights reserved.
doi:10.1016/j.tox.2011.01.015

noninvasive optical access to the vasculature and continuous monitoring of vascular functions. Moreover, Manabe et al. injected QD-conjugated captopril (anti-hypertensive drug) into stroke-prone spontaneously hypertensive rats (SHRSP) and analyzed the kinetics and dynamics of such QD-conjugated captopril (Manabe et al., 2006). QDs therefore appear to be a powerful tool for elucidating the pharmacokinetics and pharmacodynamics of drug candidates. However, these novel techniques raised concerns about QDs toxicity on the toxin-susceptible vascular system, especially on the endothelium. Because QDs are need to be directly injected into vascular for these applications, and thus may interact with and impair vascular endothelial cells (ECs), which line the luminal surface of all blood vessels.

The vascular ECs represent a dynamic interface between the circulatory system and the nonvascular tissues, and therefore protect nonvascular tissues such as brain from harmful substances (Lum and Malik, 1994). Besides their barrier function, they also play an important role in maintaining vascular homeostasis by releasing various factors to influence vascular tone, thrombogenesis, inflammation, and vessel growth and remodeling (Cines et al., 1998). Endothelial dysfunction and/or apoptosis, whether caused by physical injury or toxicants-induced cellular damage, are considered as early pathological features and independent predictors of poor prognosis in most forms of cardiovascular diseases (CVDs) (Choy et al., 2001; Halcox et al., 2002). Hence, the potential injuries of vascular ECs by QDs are expected to be cardiovascular risks for human. Furthermore, because mitochondrion is a key organelle in conversion of energy, regulation of cellular signaling as well as amplification of programmed cell death in eukaryotic cells including ECs (Duchen, 1999), mitochondrial impairment is believed to induce endothelial dysfunction and promote a series of processes that initiate and exacerbate atherosclerosis (Davidson and Duchen, 2007). Previous studies have shown that mitochondria participate in the QDs-induced apoptotic insults to several cell types (Lovric et al., 2005b; Choi et al., 2007). However, the questions of whether QDs can directly affect mitochondrial functions, activate mitochondrial death pathways or even trigger apoptosis in ECs remain unanswered.

In this study, we synthesized mercaptosuccinic acid (MSA)-capped CdTe QDs directly in aqueous condition, and investigated the direct effects of these CdTe QDs on endothelial injury, especially focusing on mitochondrial function and apoptosis. MSA-capped CdTe QDs were selected for this study because they have narrow band gaps and wide Bohr exciton radius, which equip them smaller sizes than most of CdSe QDs for red or near infrared (NIR) emission (Yu et al., 2003). These features enable CdTe QDs with different emission spectra tuned in a broader range can be effectively resolved over the same size range. Our QDs also have favorable pH-stability which supported resistance to the degradation under complicated biological environments. HUVECs were selected in our experiments as an *in vitro* model to assess the vascular toxicity of CdTe QDs. These studies should provide insight into the cardiovascular risk induced by QDs in circulation and the helpful guidance on the future safe use of QDs. Understanding the mechanisms underlying QD-toxicity will also help researchers improve the eventual design and manipulation of QDs to make them more suitable tools in nanomedicine.

2. Materials and methods

2.1. Chemicals and materials

Cadmium chloride ($CdCl_2$, 99.0%), tellurium powder (Te, 99.5%) were from Alfa Aesar (London, UK). Sodium borohydride (96%), hydrochloric acid (HCl) and sodium hydroxide (NaOH) were from Sinopharm Chemical Reagent Co., Ltd. (Shanghai, China). All chemicals were used without further purification. Solutions were prepared using Milli-Q water (Millipore) as the solvent. MSA was from Sigma-Aldrich Crop. (St. Louis, USA). Water-soluble (carboxyl coated) CdTe quantum dots were purchased from ZhongDS (Shenzhen, China) (referred to as commercial QDs).

Medium 200 (M200), low serum growth supplement (LSGS), fetal bovine serum (FBS), calcein-AM, Vybrant® Apoptosis Assay Kit, MitoTracker Red FM and 5,5′,6,6′-tetrachloro-1,1′,3,3′-tetraethylbenzimidazolylcarbocyanine iodide (JC-1) were from Invitrogen Corp. (Carlsbad, USA). The antibodies including anti-human Bcl-2, anti-human Bax, anti-human cytochrome *c*, anti-human caspase-9 and anti-human caspase-3 were from Santa Cruz Biotechnology (Santa Cruz, USA). The reactive oxygen species (ROS) assay kit (containing 2′,7′-dichlorfluorescein-diacetate, DCFH-DA, and positive control agent Rosup) as well as N-acetylcysteine (NAC) were purchased from Beyotime Institute of Biotechnology (Jiangsu, China). The 3,3,5,5-tetramethylbenzidine (TMB) Liquid Substrate kit was from Amresco, Inc. (Solon, USA). The secondary antibodies and other biological reagents were from Sigma-Aldrich Crop. (St. Louis, USA).

2.2. Preparation and characterization of quantum dots

The CdTe QDs were synthesized based on the reaction of $CdCl_2$ and NaHTe solution with MSA as surfactant (Fu et al., 2010). First, Cd^{2+}-MSA precursor solution was prepared by dissolving $CdCl_2$ (0.184 g) and MSA (0.183 g) in 60 mL deionized ultra-pure water. The pH of the solution was adjusted to 6.5 using 1 M NaOH solution. This mixture was degassed and kept stirring at room temperature. Then, NaHTe solution (4 mL, 0.05 mM), which was prepared by dissolving Te powder in $NaBH_4$ solution, was injected into the precursor solution. The reaction between cadmium ions and NaHTe took place immediately after the injection of NaHTe and the color of the solution turned red instantly. The molar ratio of Cd^{2+}:NaHTe:MSA was 1:0.2:1.2. Next, the CdTe precursor crude solution was refluxed under open-air condition at 100 °C. The as-prepared QDs were precipitated with an equivalent amount of 2-propanol, and then resuspended in water and precipitated with 2-propanol three more times. The pellet of purified QDs was dried overnight at room temperature in vacuum, and the final product in the powder form could be redissolved in water. Stock solutions of QDs for our following biological experiments were prepared by dissolving CdTe QDs in sterilized phosphate buffered saline (PBS, pH 7.4) and filter sterilized through 0.22 μm filter.

The high resolution transmission electron microscopy (HRTEM) image was taken by a JEM 2010 microscope (JEOL, Japan) with an acceleration voltage of 200 kV. The absorption spectrum and emission spectrum were recorded with a UV2550 scanning spectrophotometer (Shimadzu, Japan) and an F-2500 Spectrofluorometer (Hitachi, Japan), respectively. To measure their photostability in physiological environment and weak acidic environment, our as-prepared QDs and a similar commercial CdTe QDs were dissolved in deionized ultra-pure water with the pH value adjusted to 7.4 or 5.0 with NaOH or HCl, respectively. Then the QD solutions were added into the microplate and their emission peak intensities were measured at 405 nm excitation and 599 nm emission every 20 min during 15 h periods with a fluorescence microplate reader (Flexstation 3, Molecular Device). To determine the composition of MSA-capped CdTe QDs, the concentration of mercaptosuccinate capping ligands was determined by measuring the total organic carbon (TOC, TOC-VCPH, Shimadzu, Japan). The concentration of cadmium from QDs was measured by graphite furnace atomic absorption spectroscopy (GFAA, AA800 Spectrometer, Thermo Scientific). To measure the free cadmium ions released from CdTe QDs, 2 mL CdTe QDs stock solution (1 mg/mL) was added into dialysis tube (molecular-weight cutoff of 400 Da, MWCO-400, 3M Co. Ltd.) and then placed in polypropylene beakers containing 500 mL ultra pure water. The dialysis experiment lasted for 30 h, and 2 mL dialysis solution was taken at the 6th, 18th and 30th hour. Finally, the collected samples were analyzed using GFAA. All the measurements were performed at room temperature and in triplicate.

2.3. Cell culture and treatments

Primary HUVECs were obtained from human umbilical cord veins according to Ling et al. (2003). In brief, the vein was cannulated and filled with 0.1% type I collagenase. After incubation (37 °C, 15 min), the obtained pellets were centrifugated and resuspened in Medium200 with LSGS at a concentration of 10^5 cells/mL. The cells were used at passage 2–4 in our study. After reaching 90% confluence, M200 with LSGS was removed and then HUVECs were cultured with M200 (containing 2% FBS) in the presence of CdTe QDs at different final concentrations (range from 0.1 to 100 μg/mL) for 12 or 24 h. Untreated control cells were incubated with medium (also containing 2% FBS) alone.

2.4. Cell viability assessment

The viability of HUVECs treated with CdTe QDs was estimated with both 3-(4,5-dimethylthiazolyl-2)-2,5-diphenyltetrazolium bromide (MTT) (Andersson et al., 2009) and calcein ester green fluorescence assays. For the MTT assay, after reaching 90% confluence, culture medium was removed and then HUVECs in 96-well culture plates were cultured with M200 (containing 2% FBS) in the presence of CdTe QDs at a concentration gradient of 0.1–100 μg/mL for 24 h. Then, the medium was removed; 150 μL MTT solutions (0.5 mg/mL) was added to each well and incubated for another 4 h. The amount of viable cells in each well was determined by the absorbance of solubilized formazan. The optical density (O.D.) was measured at

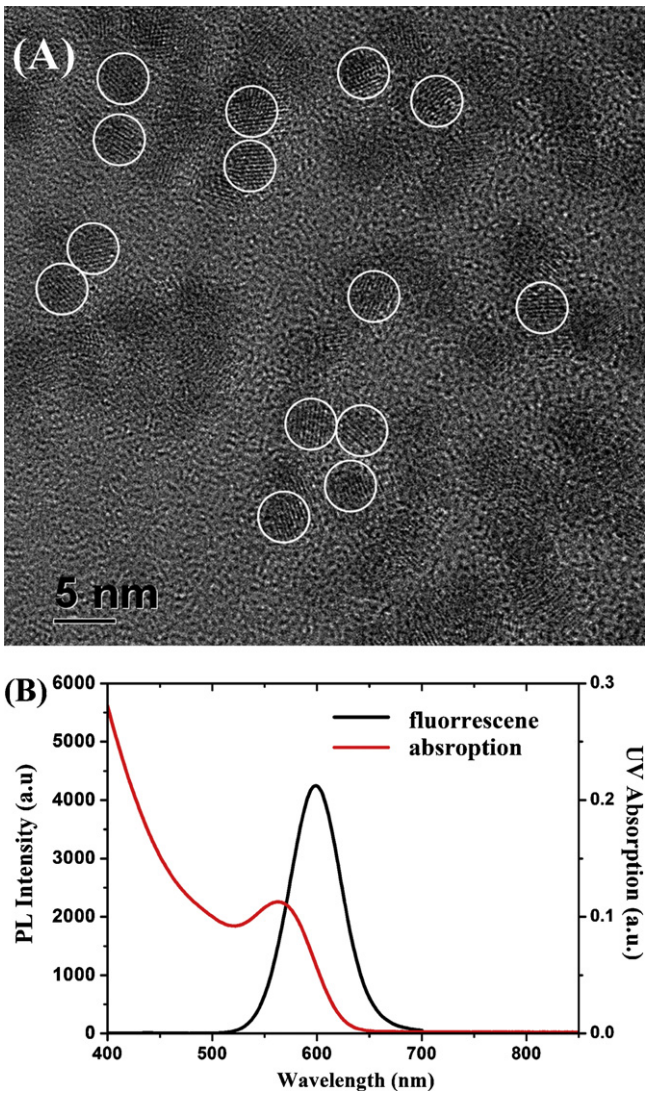

Fig. 1. MSA-capped CdTe QDs characterizations. (A) HRTEM of CdTe QDs; (B) absorption and PL spectrum of CdTe QDs. Bar = 5 nm.

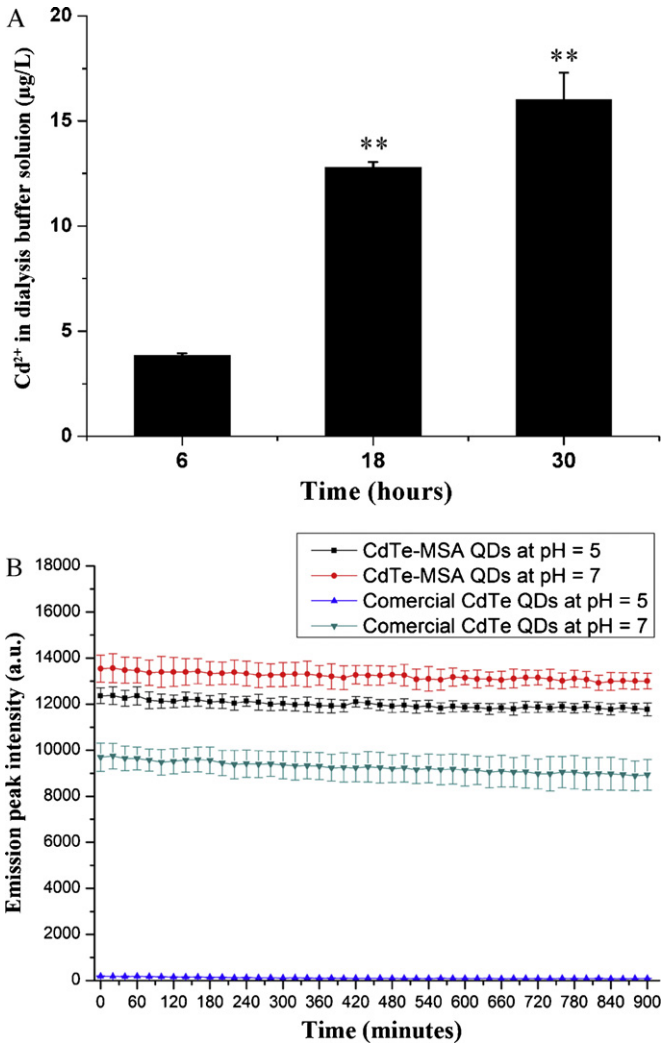

Fig. 2. MSA-capped CdTe QDs characterizations. (A) The concentration of free Cd^{2+} in the dialysis buffer solution; (B) the emission peak intensity of CdTe QDs solution with different pH values were measured at 405 nm excitation and 599 nm emission every 20 min for 15 h periods with a fluorescence microplate reader (mean ± SD, $n = 4$).

490 nm with a microplate reader (Versa Max, Molecular Devices). For using a calcein ester green fluorescence assay, cells were washed with PBS twice after the treatment with QDs and incubated with 2 μM calcein-AM for 10 min. The fluorescence images of cells were obtained with a laser scanning confocal microscope (LSM 510, Carl Zeiss).

2.5. Detection of cellular apoptosis

Exposed membrane phosphatidylserine (PS) in apoptotic cells induced by QDs was identified by flow cytometry (FCM) using a commercial apoptosis detection kit (Vybrant® Apoptosis Assay Kit, Invitrogen), according to Hsiao et al. (2009). In brief, after 90% confluence, HUVECs were cultured with M200 (containing 2% FBS) in the presence of 0.1–10 μg/mL CdTe QDs for 24 h. The treated cells were rinsed twice with PBS, harvested by trypsinization, and labeled with 5 μg/mL FITC-conjugated Annexin-V for 15 min. The fluorescence of Annexin-V-positive HUVECs was measured with FACScalibur flow cytometer (Becton Dickinson, USA) on the FL-1 detector (530 ± 15 nm, band pass). For statistical significance, at least 10,000 cells were analyzed in each sample.

The involvement of ROS in CdTe QDs-induced apoptosis was also examined by this FCM assay. HUVECs were pre-incubated with a ROS scavenger NAC (1 mM) for 2 h; and then with or without a QDs suspension (10 μg/mL) for an additional 24 h. To study whether CdTe QDs-induced apoptosis in HUVECs was caspase-dependent, caspase inhibitors Z-VAD-FMK (50 μM) or Ac-DEVD-CHO (20 mM) were incubated with HUVECs for 1 h prior to the addition of QDs (10 μg/mL). Then, after treatment, the apoptotic HUVECs were also detected on the FL-1 detector of the FACScalibur flow cytometer.

2.6. Evaluation of intracellular ROS and mitochondrial membrane potential ($\Delta\psi_m$)

DCFH-DA was used for ROS detection. DCFH-DA is transported across the cell membrane and cleaved by nonspecific esterases to form DCFH, which is further oxidized by ROS to form the fluorescent compound DCF. HUVECs were rinsed twice with PBS, trypsinized and stained with DCFH-DA (5 μM) after 12 or 24 h QDs treatment. The green fluorescence of DCF was detected on the FL1 detectors in a FACScalibur flow cytometer. HUVECs stimulated with Rosup (50 μg/mL) for 30 min were taken as positive controls of ROS generation. To explore the effect of NAC on potential ROS elevation which caused by CdTe QDs, HUVECs were pre-incubated with 0.1, 1 or 10 mM NAC for 2 h and then treated with 1 μg/mL CdTe QDs for another 24 h. The DCF fluorescence intensity was also measured with flow cytometry.

For quantitative analysis of $\Delta\psi_m$, QDs-treated HUVECs were also rinsed twice with PBS, trypsinized and then stained with JC-1. JC-1 is a lipophilic probe which potential-dependently accumulated in mitochondria and its fluorescence emission shifts from red (~590 nm, J-aggregates) to green (~525 nm, J-monomers) when $\Delta\psi_m$ decreases. The fluorescence of J-monomers was quantified on FL1 detector of FACScalibur flow cytometer. The negative control for flow cytometer compensation was prepared by addition of $\Delta\psi_m$ disrupter m-chlorophenyl-hydrazone (CCCP, 50 μM) to untreated HUVECs for the complete mitochondrial depolarization. To further clarify the role of QDs-caused ROS in induction of mitochondrial depolarization, HUVECs were pre-incubated with NAC (1 mM) for 2 h and then with or without a QDs suspension (10 μg/mL) for an additional 24 h. Subsequently, the cells were rinsed, trypsinized, loaded with JC-1 and analyzed by flow cytometer. For statistical significance, at least 10,000 cells were analyzed in each sample.

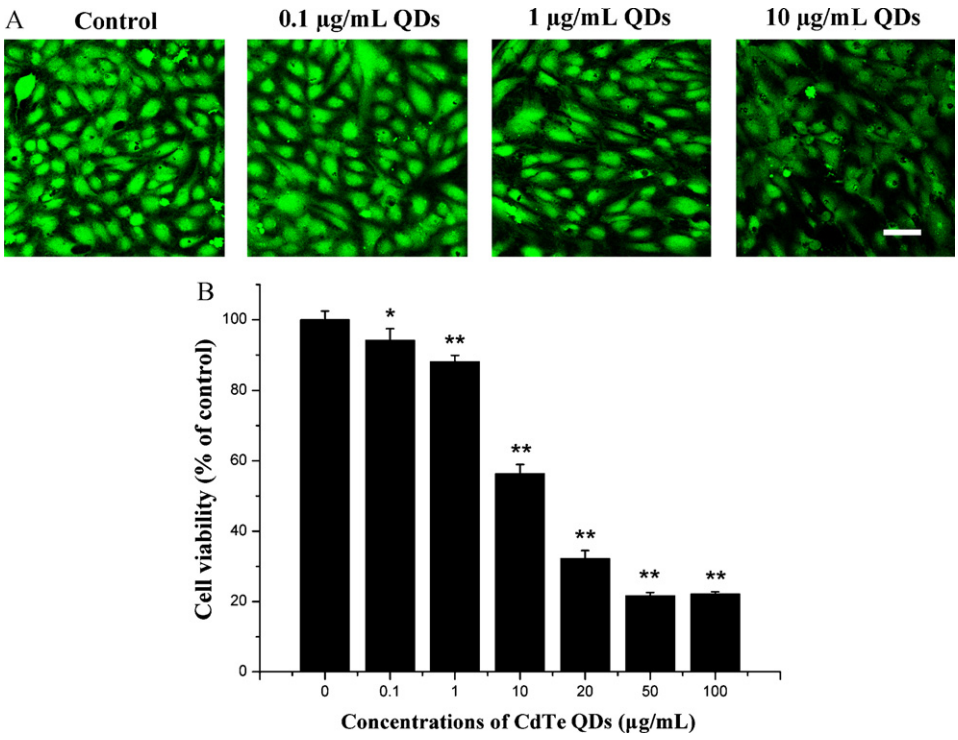

Fig. 3. CdTe QDs caused decline of cell viability in HUVECs. HUVECs were treated with various concentrations of QDs for 24 h. Cell viability measured by (A) Calcein-AM fluorescence staining; and (B) MTT assay. Data represent mean ± SD of four determinations. $^{*}p < 0.05$ and $^{**}p < 0.01$ compared with control. Bars = 50 μm.

2.7. Visualization of mitochondria structure

To examine mitochondrial structure in HUVECs treated with QDs for 24 h, MitoTracker Red FM (0.1 μM) was added after twice PBS washing. After a short incubation period of 15 min, the fluorescence images of mitochondria were obtained using a LSM510 laser scanning confocal microscope (Carl Zeiss, Germany).

2.8. Cytochrome c immunostaining in QDs-treated HUVECs

The release of cytochrome *c* from mitochondria was detected using immunostaining analysis. Briefly, HUVECs were washed twice with PBS and loaded with 100 nM MitoTracker Red FM for 20 min after 24 h QDs treatment. Then, cells were fixed with 3.7% paraformaldehyde and permeabilized for immunostaining. Mouse polyclonal anti-cytochrome *c* (1:200) and FITC-conjugated mouse IgG (1:500) were used. The translocation of cytochrome *c* from mitochondria to cytoplasm was observed by a Carl-Zeiss LSM 510 confocal laser microscope.

2.9. Immunoblot analysis of cellular expression of apoptotic proteins

HUVECs exposed to CdTe QDs for 24 h were rinsed with cold PBS and lysed for 30 min in cold radioimmune precipitation assay (RIPA) buffer (1% Triton X-100, 50 mM Tris/HCl, pH 7.4, 300 mM NaCl, 10 μg/mL aprotinin, 10 μg/mL leupeptin, 1 mM sodium orthovanadate, and 2 mg/mL iodoacetamide). After removing cellular debris by centrifugation (13,000 rpm, 10 min, 4 °C), the cell lysates were subjected to 12% sodium dodecyl sulfate polyacrylamide gel electrophoresis (SDS–PAGE) and subsequently transferred onto polyvinylidene difluoride (PVDF) membranes (Millipore). Blocking of unspecific binding sites with nonfat dry milk (5% in Tris-buffered saline containing 0.1% Tween-20) was followed by incubation with primary antibodies (Bcl-2 1:500; Bax 1:1000; caspase-9 1:500; caspase-3 1:1000), which were detected with horseradish peroxidase (HRP)-conjugated secondary antibodies, using a TMB Liquid Substrate kit.

2.10. Statistical analysis

Experiments were performed at least three times. Data were presented as mean ± SD and evaluated for statistical significance by one- or two-way analysis of variance, followed by a *post hoc* test.

3. Results

3.1. Characterizations of CdTe QDs

HRTEM images (Fig. 1A) showed that the CdTe QDs as-prepared have a highly crystalline nature and a very uniform size (~4 nm). The typical visible absorption and photoluminescence (PL) spectrum of CdTe QDs in Fig. 1B showed that the QDs has a narrow, symmetric emission spectrum (about 60 nm full width at half maximum, FWHM) and the emission peak at 599 nm. According to Yu et al. (2003), we calculated the diameter and concentration of QDs from UV–visible absorption spectrum. For the as-prepared CdTe QDs, the diameter of QDs was about 3.36 nm; and the molarity of 10 μg/mL stock solution was about 22.7 nM.

In this study, we used MSA as the surface coating to protect the QDs core. The concentration of mercaptosuccinate capping ligands was assessed by measuring the TOC. The TOC content in 10 μg/mL QDs stock solution was about 0.686 ± 0.03 μg/mL. Because the TOC in mercaptosuccinate ($C_4H_5O_4S^-$) was about 32% of the total mass, the content of MSA can be calculated as 2.14 ± 0.03 μg/mL. On the other hand, the concentration of Cd from the 10 μg/mL QDs stock solution was determined as 5.77 ± 0.16 μg/mL by GFAA. Based on these results above, the formula $Cd_{10}Te_{3.18}(SCH_2CHCOOHCOOH)_{2.78}$ is suggested. Respecting the instrument error and the surface-to-volume atom ratio (Peng and Peng, 2002; Yu et al., 2003), our results indicated that the CdTe core QDs were well capped with MSA, which was further confirmed by the free cadmium ion assays (Fig. 2A). After dialysis of 1 mg/mL CdTe QDs for 30 h, the Cd^{2+} in the dialysis buffer solution was only 15.99 ± 1.30 ng/mL, suggesting there was only a small amount of Cd^{2+} leakage from the MSA-capped CdTe QDs. Furthermore, Fig. 2B showed that the emission peak intensity of MSA-capped CdTe QDs under a weak acidic condition (pH 5) were slightly lower than that under a physiological

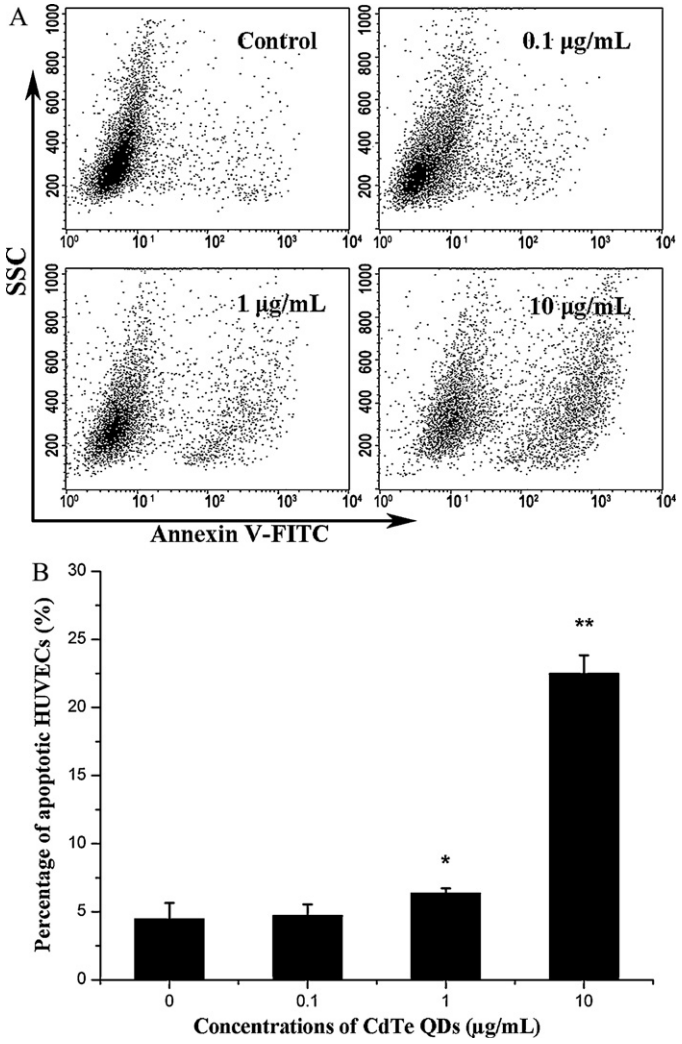

Fig. 4. CdTe QDs caused apoptosis of HUVECs. (A) PS exposure resulting from 24 h CdTe QDs treatment, HUVECs were stained with FITC conjugated Annexin-V and subjected to cytoflurometric analysis. (B) Quantitation of data obtained in (A) and parallel samples. Data represent mean ± SD of four determinations. $^{*}p < 0.05$ and $^{**}p < 0.01$ compared with control.

condition (pH 7.4) through the tested period. But the commercial carboxyl coated CdTe QDs completely lose its fluorescence when the pH value was adjusted to 5. Hence, our MSA-capped CdTe QDs have favorable properties of being water-soluble and highly pH stable, and present promising prospects in the biomedical applications.

3.2. CdTe QDs decreases cell viability of HUVECs in a dose-dependent manner

To examine the direct toxic effects on vascular ECs, cultured HUVECs were treated with CdTe QDs for 24 h. As shown in Fig. 3A, CdTe QDs dose-dependently decreased the cell viability of HUVECs, as a gradual decline in cellular calcein fluorescence was observed in the presence of 0.1–10 μg/mL CdTe QDs. MTT assay showed that significant cell death was observed with CdTe QDs at a concentration of 1 μg/mL and above (Fig. 3B, $p < 0.01$, one-way ANOVA). The TC_{50} value (concentration of CdTe QDs causes 50% cell death) was found at 10.60 μg/mL (about 24.06 nM) determined by log–logit transformation, indicating the remarkable endothelial toxicity of CdTe QDs.

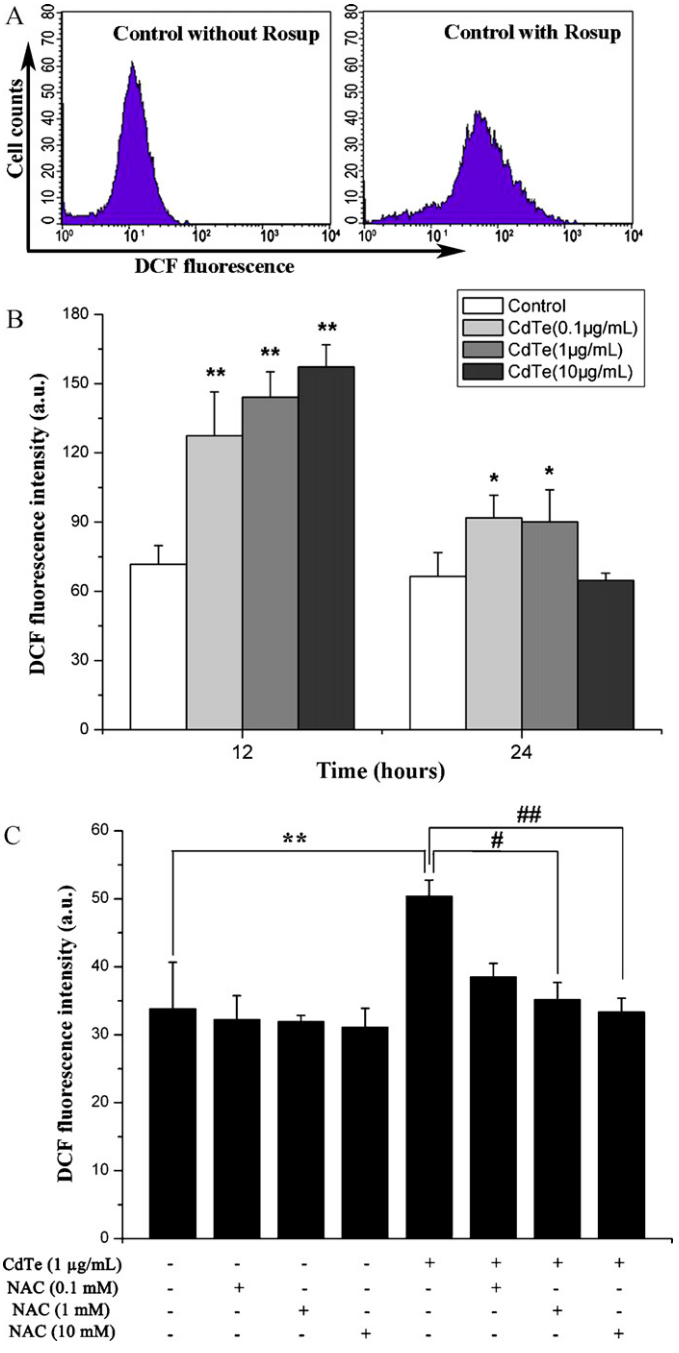

Fig. 5. Effect of CdTe QDs on ROS levels in HUVECs. (A) HUVECs stimulated with Rosup (50 μg/mL) for 30 min were taken as positive control; (B) the DCF mean fluorescence intensity of HUVECs treated with or without CdTe QDs were determined by flow cytometer; (C) the Inhibitory effects of NAC on CdTe QDs-induced ROS up-regulation in HUVECs. Data represent mean ± SD of six determinations. $^{*}p < 0.05$ and $^{**}p < 0.01$ compared with control; $^{\#}p < 0.05$ and $^{\#\#}p < 0.01$ compared with CdTe QDs-treated HUVECs.

3.3. CdTe QDs lead to apoptotic cell death of HUVECs

To further assess the extent of QDs-induced injuries, we detected the apoptosis in QDs-treated HUVECs by flow cytometry, using an Annexin-V apoptosis detection kit. The translocation of PS from the inter leaflet of the plasma membrane to outer leaflet, and then can be labeled by Annexin-V, is one of the typical features of cells undergoing apoptosis process. After 24 h incubation with QDs, the percentages of Annexin-V-positive HUVECs (Fig. 4) increased gradually depending on CdTe QDs concentration (4.48 ± 1.17% at

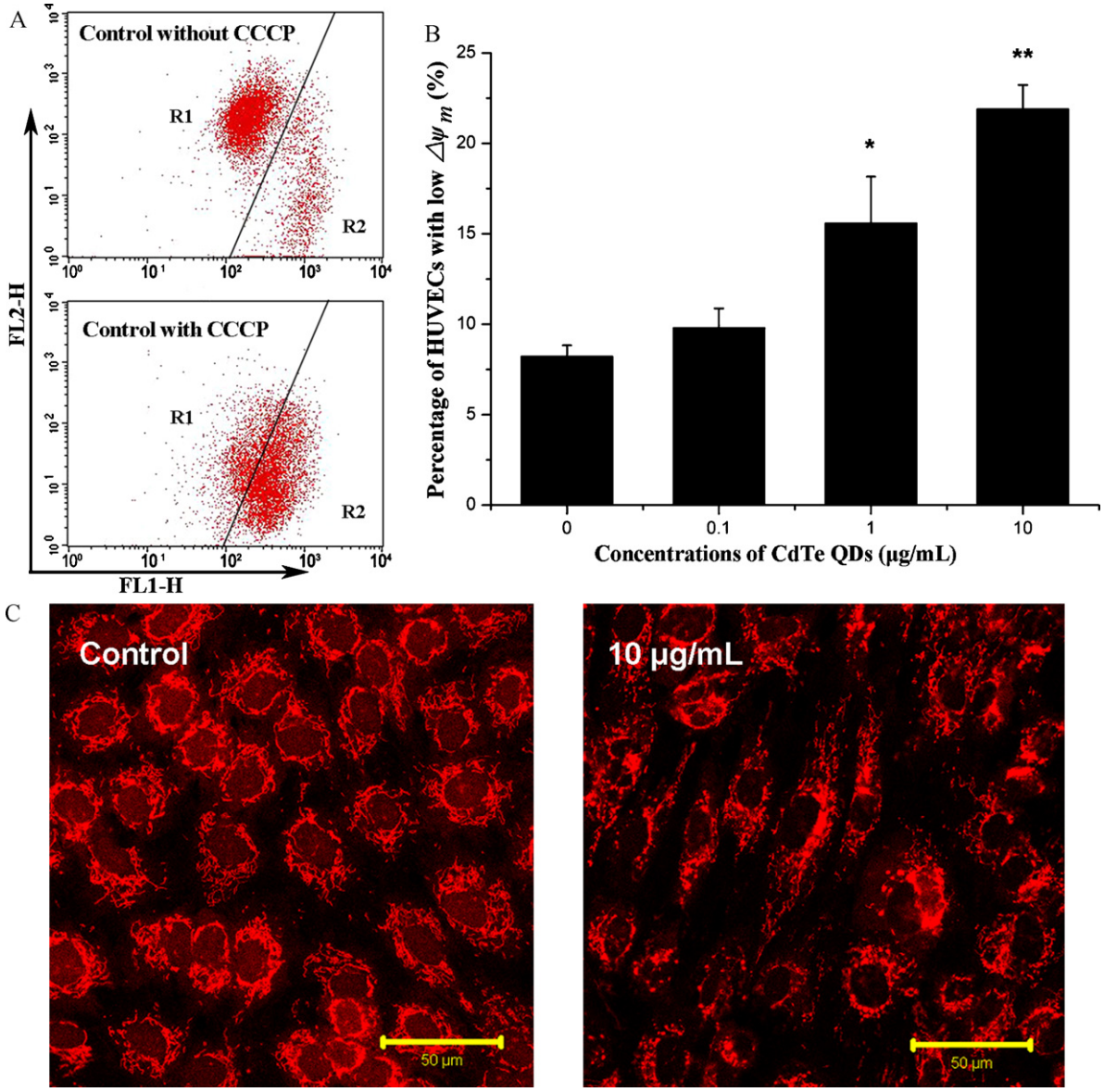

Fig. 6. Effect of CdTe QDs on mitochondrial function in HUVECs. (A) Increase of the fluorescence of J-monomers after addition of CCCP to untreated HUVECs which were labeled with JC-1 as positive control (R1: gated the healthy HUVECs with J-aggregates, R2: gated the unhealthy HUVECs with J-monomers); (B) the percentages of HUVECs with low $\Delta\psi_m$ after QDs treatment were detected by flow cytometer; (C) visualization of mitochondrial structures. Cells are stained with Mitotracker Red FM and the morphological changes of mitochondria were observed by confocal microscopy. Data represent mean ± SD of six determinations. $^{*}p < 0.05$ and $^{**}p < 0.01$ compared with control. Bars = 50 μm.

control, 4.73 ± 0.81% at 0.1 μg/mL, 6.37 ± 0.35% at 1 μg/mL and 22.49 ± 1.34% at 10 μg/mL, $p < 0.01$, one-way ANOVA). These results suggested that CdTe QDs could induce rapid apoptosis of HUVECs, and exerted direct pro-apoptotic effects in a dose-dependent manner.

3.4. CdTe QDs elevate intracellular ROS levels and subsequent mitochondrial dysfunction in HUVECs

The effect of QDs on ROS generation in HUVECs was assessed by measuring the oxidation of DCFH-DA to DCF using flow cytometer. The exposure of HUVECs to CdTe QDs for 12 h resulted in a dose-dependent increase of intracellular ROS (Fig. 5B). Compared with control, 0.1, 1 and 10 μg/mL CdTe QDs significantly promoted ROS generation by 77.76%, 100.97% and 119.35% in HUVECs, respectively ($p < 0.05$, one-way ANOVA). However, the intracellular ROS content was gradually increased to 138.10% of control at 0.1 μg/mL and 135.63% of control at 1 μg/mL after 24 h incubation, and it even restored to 2.63% lower than the control value at 10 μg/mL group (Fig. 5A). However, the elevation of intracellular ROS caused by 24 h incubation with 1 μg/mL CdTe QDs was inhibited by preincubation with NAC, which was also slightly prevented the spontaneous ROS generation (Fig. 5C). The DCF fluorescence in 1 or 10 mM NAC-pre-incubated group was significantly reduced to 69.78% or 66.17% of that in CdTe QDs-treated group. Taking together, these results revealed that CdTe QDs-induced increase of intracellular ROS production may be earlier than the apoptosis, suggesting ROS might play a role in CdTe QDs-induced apoptosis of HUVECs.

Since oxidative stress is known to impair mitochondria, whose functions are essential for maintaining cellular homeostasis, we studied the effect of CdTe QDs on $\Delta\psi_m$ and the morphology of mitochondria in HUVECs. The flow cytometric analysis (Fig. 6B) showed that incubation of HUVECs with 0.1 μg/mL CdTe QDs had no visible effect on cellular $\Delta\psi_m$. However, a higher concentration of CdTe QDs caused a pronounced reduction of $\Delta\psi_m$, as the percentage of unhealthy HUVECs with low $\Delta\psi_m$ was remarkably

increased by 89.77% or 166.41% in the presence of 1 or 10 μg/mL CdTe QDs, respectively ($p < 0.05$, one-way ANOVA). In addition, the CdTe QDs induced cytotoxic morphological changes of mitochondria in HUVECs (Fig. 6C), converting the mitochondrial tubular shape to a spherical conformation after 24 h exposure to 10 μg/mL CdTe QDs. These results suggested that CdTe QDs could induce severe impairments of mitochondria including its fragmentation and depolarization.

Moreover, we use the ROS scavenger NAC to clarify the role of ROS in CdTe QDs-induced mitochondrial impairment and apoptosis in HUVECs. As shown in Fig. 7A, NAC did not affect the maintenance of $\Delta\psi_m$ in HUVECs; but it could effectively protect HUVECs from CdTe QDs-induced disruption of $\Delta\psi_m$ – the ratio of HUVECs with low $\Delta\psi_m$ reduced by 40.46% in the presence of 1 mM NAC. The FCM data (Fig. 7B) also confirmed that NAC could markedly inhibit the CdTe QDs-induced endothelial apoptosis without adverse effect on control group; the percentage of apoptosis in both QDs and NAC co-treated HUVECs was reduced by 57.21% than that in QDs group. Altogether, these data indicated that QDs-caused intracellular ROS elevation was directly involved not only in the QDs-induced mitochondrial injury but also in QDs-induced apoptosis.

3.5. CdTe QDs activated the mitochondrial apoptotic pathways in HUVECs

Besides maintaining cellular metabolism, mitochondria have also been shown to fulfill very important functions in the signal transduction for apoptosis. Therefore, to further investigate the molecular mechanism of CdTe QDs-induced HUVECs apoptosis, we detected the expression of mitochondrial apoptosis regulatory proteins by immunoblotting analysis. The expression level of the pro-survival Bcl-2 in HUVECs dramatically decreased, whereas the level of the pro-apoptotic Bax significantly increased after 24 h of treatment (Fig. 9A). Because Bax is involved in release of cytochrome *c*, which subsequently triggers activation of caspase proteases and death of a cell by apoptosis, we then examined the subcellular distribution of cytochrome *c* by immunofluorescence. Cytochrome *c*, as a component of the electron transport chain, is found loosely associated with the inner membrane of the mitochondrion. Indeed, in control cells, the cytochrome *c* (green, Fig. 8A) showed punctuate staining in the cytoplasm/perinuclear region, and it was well co-localized with the mitochondria (red, Fig. 8B and C). In contrast, when the HUVECs treated with 10 μg/mL CdTe QDs for 24 h, the staining for cytochrome *c* in those cells was not punc-

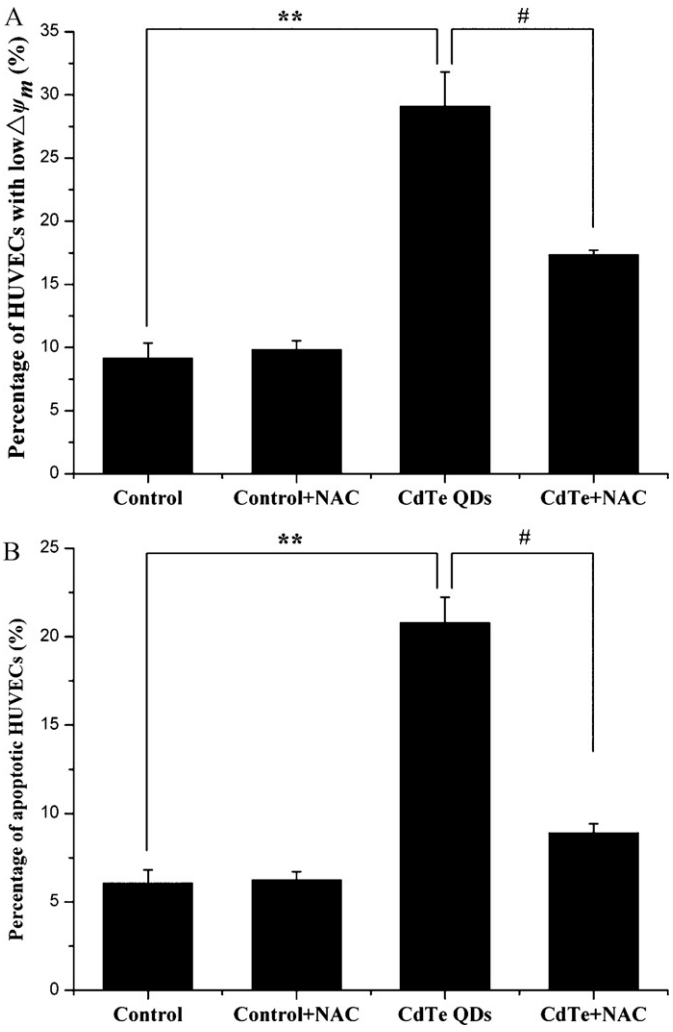

Fig. 7. The ROS scavenger NAC inhibited the CdTe QDs-induced (A) mitochondrial depolarization and (B) apoptosis of HUVECs. Data were represented as mean ± SD of six determinations. $^{**}p < 0.01$ compared with control and $^{\#}p < 0.01$ compared with CdTe QDs-treated HUVECs.

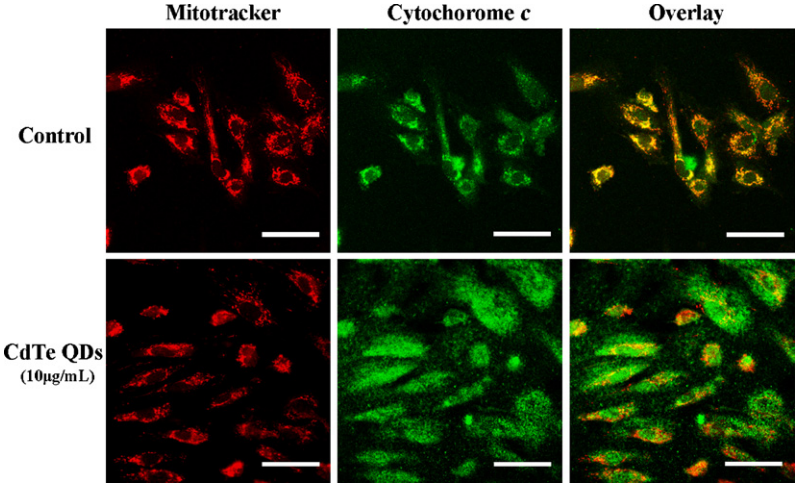

Fig. 8. Detection of cytochrome *c* leakage after 24 h CdTe QDs treatment. Double-labeling immunofluorescence staining of cytochrome *c* (the first column) and mitochondria (the first column) under normal and 10 μg/mL CdTe QDs treated conditions. Bars = 50 μm. (For interpretation of the references to colour in this figure legend, the reader is referred to the web version of the article.)

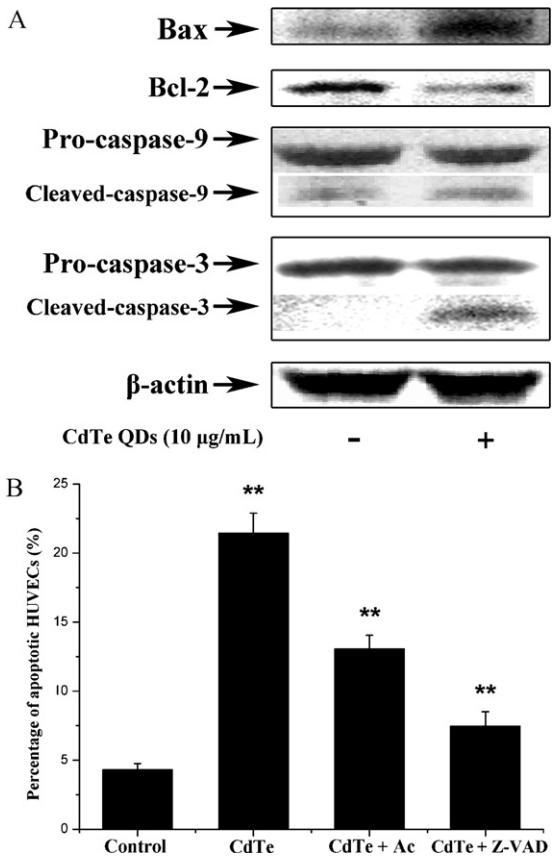

Fig. 9. CdTe QDs induce activation of mitochondrial apoptotic pathways. (A) Representative immunoblotting of Bax, Bcl-2, procaspase-9/activated caspase-9 and procaspase-3/activated caspase-3 proteins in HUVECs from both control and 10 μg/mL CdTe QDs-treated groups. (B) The inhibition of Z-VAD-FMK and Ac-DEVE-CHO in CdTe QDs-induced apoptosis of HUVECs. Data were represented as mean ± SD of six determinations. $^{**}p < 0.01$ compared with control.

tate and perinuclear but, rather, diffuse (Fig. 8E). There was scarce overlay with mitochondria can be observed in QDs-treated HUVECs (Fig. 8D and F), suggesting that the bulk of cytochrome *c* leaked from endothelial mitochondria after QDs treatment. Collectively, these results indicated that the protein expression of pro-apoptotic molecules increased in CdTe QDs-treated HUVECs.

The initiator caspase-9 and effector caspase-3, which play vital roles in the mitochondrial-dependent apoptotic pathway of cells, were both activated in HUVECs following treatment with CdTe QDs, because the immumoblotting analysis showed that the cleavage of both caspase-9 and caspase-3 could be detected after 24 h CdTe QDs treatment (Fig. 9A). The pan-caspase inhibitor Z-VAD-FMK and specific caspase-3 inhibitors Ac-DEVD-CHO were used to analyze the involvement of caspases in CdTe QDs-induced apoptosis in HUVECs. As shown in Fig. 9B, the pre-treatment of HUVECs with either Z-VAD-FMK or Ac-DEVD-CHO significantly decreased CdTe QDs-induced apoptosis to 7.48 ± 1.03% and 13.07 ± 0.98%. Taken together, our results showed that CdTe QDs directly activated the intrinsic mitochondrial apoptosis pathway in HUVECs, and this apoptotic process was clearly caspase-dependent.

4. Discussion

The present study demonstrated that MSA-capped CdTe QDs directly caused cytotoxic injury of human vascular ECs. Treatment HUVECs with the CdTe QDs significantly elevated intracellular ROS, induced widespread mitochondrial dysfunction, activated the mitochondrial apoptosis pathway, and ultimately triggered apoptotic cell death in HUVECs. These results provided strong evidences for the direct effects of QDs on vascular ECs as well as the molecular mechanisms of QDs-induced endothelial cytotoxicity.

Semiconductor QDs have attracted great concern as novel fluorophores for labeling cells or tissues and drug tracing during the last decade (Jaiswal et al., 2003; Medintz et al., 2005). CdTe QDs, with narrow band gaps and wide Bohr exciton radius, have smaller sizes than most of commercial CdSe QDs at the red or near infrared (NIR) range; and thus they can be effectively resolved over the same size range. Besides that, our data of element composition determination and Cd^{2+} leakage assay confirmed that our CdTe core QDs was well capped with MSA, which was reported to provide more excellent stabilities of QDs against aggregation at low pH than mostly employed mercaptoacetic acid (MPA) or dihydrolipoic acid (DHLA) (Algar and Krull, 2007). In fact, our as-prepared QDs have efficient luminescence, and they do have higher pH stability (Fig. 2B) than that of a similar commercial QDs. Hence, our QDs with excellent optical properties are suitable for biomedical applications such as bioimaging, composite drug delivery or disease diagnosis agents. However, little is known about whether such QDs affect endothelial function when they enter vasculature through injection as the imaging agents. Therefore, employing HUVECs as an *in vitro* model, we explored the potential endothelial toxicity of these MSA-capped CdTe QDs.

In this study, we tested the endothelial toxicity of MSA-capped CdTe QDs in the concentration range from 0.1 to 100 μg/mL (coresp. molarity was about 0.227–227 nM). According to previous reports, the concentration which we tested in our following experiments is similar to the doses that have actually used in *in vivo* bioimaging (up to hundreds of nanomole) (Larson et al., 2003; Ballou et al., 2004, 2007; Gao et al., 2004; Cai et al., 2006; Jayagopal et al., 2007; Tada et al., 2007) or tested in other *in vitro* toxicological studies (up to hundreds of nanomole or μg/mL) (Lovric et al., 2005a; Choi et al., 2007; Tang et al., 2008; Chang et al., 2009; Su et al., 2009, 2010; Chen et al., 2010; Wu et al., 2010). Then, our cell viability assays (Fig. 3) revealed that CdTe QDs caused significant cell loss in a dose-dependent manner (at or above 0.1 μg/mL), demonstrating CdTe QDs manifested cytotoxic effect against HUVECs. Quantitive cytometric analysis disclosed that, in HUVECs, exposure to CdTe QDs induced dose-dependent apoptotic cell death (Fig. 4), which might compromise vasoregulation, increase smooth muscle cells (SMCs) proliferation and/or migration and facilitate blood clotting (Busse et al., 1985; Bombeli et al., 1997; Raymond et al., 2004), leading to CVDs such as atherosclerosis and thrombus. Notably, the concentration of CdTe QDs required to promote endothelial toxicity (TC_{50}) in our study was much lower than most of that in other cell types (Shiohara et al., 2004; Lovric et al., 2005a; Choi et al., 2007; Tang et al., 2008; Chang et al., 2009; Su et al., 2009, 2010; Chen et al., 2010; Wu et al., 2010). A possible explanation for this difference is that the tested cell types have different cellular sensitivity to QDs. In other words, vascular ECs may be more susceptible to damage by QDs.

QDs were reported to generate reactive singlet oxygen species (Samia et al., 2003). To explore if QDs could induced overabundant intracellular ROS and if QDs-induced oxidative stress was tightly associated with their endothelial toxicity (Cho et al., 2007), we measured the ROS intensity and potential injuries of mitochondrial functions in QDs-treated HUVECs. Here we observed that 12 h treatment with QDs could trigger a twofold elevation of intracellular ROS (Fig. 5), followed by obvious disruption of $\Delta\psi_m$ (Fig. 6B), as well as mitochondrial fragmentation (Fig. 6C) after another 12 h QDs incubation. Moreover, NAC, as ROS scavenger, did effectively prevent QDs-induced ROS up-regulation (Fig. 5C); and it also inhibited the QDs-induced mitochondrial depolarization or apoptosis in HUVECs (Fig. 7). Hence, considering the free Cd^{2+} released from MSA-capped CdTe QDs is little (Fig. 2A), we suppose that QDs-induced endothe-

lial toxicity was mostly mediated by elevated intracellular ROS; and mitochondria may be a major target organelle. This undesirable oxidative damage caused by QDs also reminder that the surface modification of QDs, which may reduce the production of ROS, is of crucial importance in order to prepare non-toxic fluorescent probes for future scientific and clinical usage. Meanwhile, unlike other cells, vascular ECs obtain most of their energy from anaerobic glycolysis, and the collapse of endothelial $\Delta\psi_m$ inhibits mitochondrial production of NO, which can rapidly modulate cellular functions and apoptosis (Culic et al., 1997; Dedkova et al., 2004; Quintero et al., 2006). Therefore, QDs-induced mitochondrial oxidative damage in ECs may represent an important step in the development of endothelial dysfunction *per se* rather than a key role in diminishment of cellular energy production in other cells.

On the other hand, nanomaterials-generated high level of ROS was also confirmed to lead detrimental autophagic cell death as well as necrosis (Yamawaki and Iwai, 2006; Stern et al., 2008; Liu and Sun, 2010). Our preliminary results (data not shown) revealed that 10 μg/mL CdTe QDs could convert the cytosolic protein microtubule-associated protein 1 light chain 3-I (LC3-I) to LC3-II which was associated with the formation of autophagosomes. Combing the previous reports and our data, we conjectured that autophagic and/or necrotic cell death were possibly implicated in QDs-induced endothelial damage and this could partially explain the seemingly contradictory data that the percentage of apoptotic HUVECs treated with 10 μg/mL CdTe QDs (a dose similar to the TC_{50} value determined by MTT assay) was lower than 50%. Nevertheless, the question of whether QDs directly induce autophagy or necrosis in ECs requires further investigation.

Furthermore, the present study found that QDs directly activated the intrinsic mitochondrial apoptosis pathway, which is widely involved in vascular diseases (Tanaka et al., 2003; Vindis et al., 2005; Davidson and Duchen, 2007). After 24 h incubation, CdTe QDs caused an increase of pro-apoptotic Bax but a decrease of pro-survival Bcl-2 (Fig. 9A); and they also caused the release of cytochrome *c* (Fig. 8), accompanied by the cleavage of caspase-9 and caspase-3 (Fig. 9A). Moreover, the apoptosis caused by CdTe QDs was significantly reduced by caspase inhibitors (Fig. 9B), indicating caspases are essential for CdTe QDs-induced apoptosis in ECs. It is noteworthy that our result is different from the previous study by Lovric et al., in which they observed that QDs-induced cell death was caspase-independent in cells with caspase-3 expression (PC12 cells) or without (MCF-7, a breast cancer cell line) (Lovric et al., 2005b). As the QDs used in two studies were of similar composition, the same dose (10 μg/mL) and induced similar impairments of mitochondria in all three cell types, the discrepancy of downstream apoptosis signal components of mitochondria seemed to arise from different cell types. Collectively, the understanding of the mechanism underlying QDs-induced cell death is still far from complete, and may be complicated by cell types and signaling context differences.

In conclusion, we have demonstrated that QDs increased the generation of intracellular ROS, impaired mitochondrial functions, activated the mitochondrial apoptosis pathway and finally promoted apoptotic cell death in HUVECs. Our overall findings provided strong evidence that the QDs circulating in blood was a potential significant risk factor for CVDs. With increased utilization of QDs in biomedical research as well as the potential clinical usage, these data also offer helpful guidance on future safe use of QDs and help researchers improve the manipulation of QDs to make them more suitable tools in life science.

Conflict of interest statement

The authors declare that there is no conflict of interest.

Acknowledgement

The authors acknowledge the assistance of Wanting Niu, Wei Cai and Wei Jiang for the GFAA and the TOC measurements. We would also like to thank Dr. Chuxiong Hu for his kind help during this study. The work described in this paper was supported in part by the National Natural Science Foundation of China (No. 30900301).

Appendix A. Supplementary data

The optical characters and fluorescence detection channels of different dyes used in our experiments were listed.

Supplementary data associated with this article can be found, in the online version, at doi:10.1016/j.tox.2011.01.015.

References

Algar, W.R., Krull, U.J., 2007. Luminescence and stability of aqueous thioalkyl acid capped CdSe/ZnS quantum dots correlated to ligand ionization. ChemPhysChem 8, 561–568.

Andersson, H., Piras, E., Demma, J., Hellman, B., Brittebo, E., 2009. Low levels of the air pollutant 1-nitropyrene induce DNA damage, increased levels of reactive oxygen species and endoplasmic reticulum stress in human endothelial cells. Toxicology 262, 57–64.

Bagalkot, V., Zhang, L., Levy-Nissenbaum, E., Jon, S., Kantoff, P.W., Langer, R., Farokhzad, O.C., 2007. Quantum dot – Aptamer conjugates for synchronous cancer imaging, therapy, and sensing of drug delivery based on bi-fluorescence resonance energy transfer. Nano Lett. 7, 3065–3070.

Ballou, B., Lagerholm, B.C., Ernst, L.A., Bruchez, M.P., Waggoner, A.S., 2004. Noninvasive imaging of quantum dots in mice. Bioconjugate Chem. 15, 79–86.

Ballou, B., Ernst, L.A., Andreko, S., Harper, T., Fitzpatrick, J.A.J., Waggoner, A.S., Bruchez, M.P., 2007. Sentinel lymph node imaging using quantum dots in mouse tumor models. Bioconjugate Chem. 18, 389–396.

Bombeli, T., Karsan, A., Tait, J.F., Harlan, J.M., 1997. Apoptotic vascular endothelial cells become procoagulant. Blood 89, 2429–2442.

Busse, R., Trogisch, G., Bassenge, E., 1985. The role of endothelium in the control of vascular tone. Basic Res. Cardiol. 80, 475–490.

Cai, W., Shin, D.W., Chen, K., Gheysens, O., Cao, Q., Wang, S.X., Gambhir, S.S., Chen, X., 2006. Peptide-labeled near-infrared quantum dots for imaging tumor vasculature in living subjects. Nano Lett. 6, 669–676.

Chang, S.Q., Dai, Y.D., Kang, B., Han, W., Mao, L., Chen, D., 2009. UV-enhanced cytotoxicity of thiol-capped CdTe quantum dots in human pancreatic carcinoma cells. Toxicol. Lett. 188, 104–111.

Chen, J.Y., Lee, Y.M., Zhao, D., Mak, N.K., Wong, R.N.S., Chan, W.H., Cheung, N.H., 2010. Quantum dot-mediated photoproduction of reactive oxygen species for cancer cell annihilation. Photochem. Photobiol. 86, 431–437.

Cho, S.J., Maysinger, D., Jain, M., Roder, B., Hackbarth, S., Winnik, F.M., 2007. Long-term exposure to CdTe quantum dots causes functional impairments in live cells. Langmuir 23, 1974–1980.

Choi, A.O., Cho, S.J., Desbarats, J., Lovric, J., Maysinger, D., 2007. Quantum dot-induced cell death involves Fas upregulation and lipid peroxidation in human neuroblastoma cells. J. Nanobiotechnol. 5, 1.

Choy, J.C., Granville, D.J., Hunt, D.W.C., McManus, B.M., 2001. Endothelial cell apoptosis: biochemical characteristics and potential implications for atherosclerosis. J. Mol. Cell. Cardiol. 33, 1673–1690.

Cines, D.B., Pollak, E.S., Buck, C.A., Loscalzo, J., Zimmerman, G.A., McEver, R.P., Pober, J.S., Wick, T.M., Konkle, B.A., Schwartz, B.S., Barnathan, E.S., McCrae, K.R., Hug, B.A., Schmidt, A.M., Stern, D.M., 1998. Endothelial cells in physiology and in the pathophysiology of vascular disorders. Blood 91, 3527–3561.

Coe, S., Woo, W.K., Bawendi, M., Bulovic, V., 2002. Electroluminescence from single monolayers of nanocrystals in molecular organic devices. Nature 420, 800–803.

Culic, O., Gruwel, M.L.H., Schrader, J., 1997. Energy turnover of vascular endothelial cells. Am. J. Physiol.: Cell Ph. 42, C205–C213.

Davidson, S.M., Duchen, M.R., 2007. Endothelial mitochondria – contributing to vascular function and disease. Circ. Res. 100, 1128–1141.

Dedkova, E.N., Ji, X., Lipsius, S.L., Blatter, L.A., 2004. Mitochondrial calcium uptake stimulates nitric oxide production in mitochondria of bovine vascular endothelial cells. Am. J. Physiol.: Cell Ph. 286, C406–C415.

Derfus, A.M., Chan, W.C.W., Bhatia, S.N., 2004. Probing the cytotoxicity of semiconductor quantum dots. Nano Lett. 4, 11–18.

Duchen, M.R., 1999. Contributions of mitochondria to animal physiology: from homeostatic sensor to calcium signalling and cell death. J. Physiol. 516 (Pt 1), 1–17.

Ekimov, A.I., Efros, A.L., Onushchenko, A.A., 1985. Quantum size effect in semiconductor microcrystals. Solid State Commun. 56, 921–924.

Fu, T., Qin, H.Y., Hu, H.J., Hong, Z., He, S.L., 2010. Aqueous synthesis and fluorescence-imaging application of CdTe/ZnSe core/shell quantum dots with high stability and low cytotoxicity. J. Nanosci. Nanotechnol. 10, 1741–1746.

Gao, X.H., Cui, Y.Y., Levenson, R.M., Chung, L.W.K., Nie, S.M., 2004. In vivo cancer targeting and imaging with semiconductor quantum dots. Nat. Biotechnol. 22, 969–976.

Halcox, J.P., Schenke, W.H., Zalos, G., Mincemoyer, R., Prasad, A., Waclawiw, M.A., Nour, K.R., Quyyumi, A.A., 2002. Prognostic value of coronary vascular endothelial dysfunction. Circulation 106, 653–658.

Hsiao, P.N., Chang, M.C., Cheng, W.F., Chen, C.A., Lin, H.W., Hsieh, C.Y., Sun, W.Z., 2009. Morphine induces apoptosis of human endothelial cells through nitric oxide and reactive oxygen species pathways. Toxicology 256, 83–91.

Huffaker, D.L., Park, G., Zou, Z., Shchekin, O.B., Deppe, D.G., 1998. 1.3 mu m room-temperature GaAs-based quantum-dot laser. Appl. Phys. Lett. 73, 2564–2566.

Huynh, W.U., Dittmer, J.J., Alivisatos, A.P., 2002. Hybrid nanorod-polymer solar cells. Science 295, 2425–2427.

Jaiswal, J.K., Mattoussi, H., Mauro, J.M., Simon, S.M., 2003. Long-term multiple color imaging of live cells using quantum dot bioconjugates. Nat. Biotechnol. 21, 47–51.

Jayagopal, A., Russ, P.K., Haselton, F.R., 2007. Surface engineering of quantum dots for in vivo vascular imaging. Bioconjugate Chem. 18, 1424–1433.

Larson, D.R., Zipfel, W.R., Williams, R.M., Clark, S.W., Bruchez, M.P., Wise, F.W., Webb, W.W., 2003. Water-soluble quantum dots for multiphoton fluorescence imaging in vivo. Science 300, 1434–1436.

Likharev, K.K., 1999. Single-electron devices and their applications. Proc. IEEE 87, 606–632.

Ling, X., Ye, J.F., Zheng, X.X., 2003. Dynamic investigation of leukocyte-endothelial cell adhesion interaction under fluid shear stress in vitro. Acta Biochim. Biophys. Sin. 35, 567–572.

Liu, X., Sun, J., 2010. Endothelial cells dysfunction induced by silica nanoparticles through oxidative stress via JNK/P53 and NF-kappaB pathways. Biomaterials 31, 8198–8209.

Lovric, J., Bazzi, H.S., Cuie, Y., Fortin, G.R.A., Winnik, F.M., Maysinger, D., 2005a. Differences in subcellular distribution and toxicity of green and red emitting CdTe quantum dots. J. Mol. Med. 83, 377–385.

Lovric, J., Cho, S.J., Winnik, F.M., Maysinger, D., 2005b. Unmodified cadmium telluride quantum dots induce reactive oxygen species formation leading to multiple organelle damage and cell death. Chem. Biol. 12, 1227–1234.

Lum, H., Malik, A.B., 1994. Regulation of vascular endothelial barrier function. Am. J. Physiol. Lung Cell Mol. Physiol. 267, L223–L241.

Manabe, N., Hoshino, A., Liang, Y.Q., Goto, T., Kato, N., Yamamoto, K., 2006. Quantum dot as a drug tracer in vivo. IEEE Trans. Nanobiosci. 5, 263–267.

Medintz, I.L., Uyeda, H.T., Goldman, E.R., Mattoussi, H., 2005. Quantum dot bioconjugates for imaging, labelling and sensing. Nat. Mater. 4, 435–446.

Peng, Z.A., Peng, X.G., 2002. Nearly monodisperse and shape-controlled CdSe nanocrystals via alternative routes: nucleation and growth. J. Am. Chem. Soc. 124, 3343–3353.

Quintero, M., Colombo, S.L., Godfrey, A., Moncada, S., 2006. Mitochondria as signaling organelles in the vascular endothelium. Proc. Natl. Acad. Sci. U. S. A. 103, 5379–5384.

Raymond, M.A., Desormeaux, A., Laplante, P., Vigneault, N., Filep, J.G., Landry, K., Pshezhetsky, A.V., Hebert, M.J., 2004. Apoptosis of endothelial cells triggers a caspase-dependent anti-apoptotic paracrine loop active on vascular smooth muscle cells. FASEB J. 18, 705.

Resch-Genger, U., Grabolle, M., Cavaliere-Jaricot, S., Nitschke, R., Nann, T., 2008. Quantum dots versus organic dyes as fluorescent labels. Nat. Methods 5, 763–775.

Rossetti, R., Nakahara, S., Brus, L.E., 1983. Quantum size effects in the redox potentials, resonance Raman-spectra and electronic-spectra of Cds crystallites in aqueous-solution. J. Chem. Phys. 79, 1086–1088.

Samia, A.C.S., Chen, X.B., Burda, C., 2003. Semiconductor quantum dots for photodynamic therapy. J. Am. Chem. Soc. 125, 15736–15737.

Shiohara, A., Hoshino, A., Hanaki, K., Suzuki, K., Yamamoto, K., 2004. On the cytotoxicity caused by quantum dots. Microbiol. Immunol. 48, 669–675.

Stern, S.T., Zolnik, B.S., McLeland, C.B., Clogston, J., Zheng, J.W., McNeil, S.E., 2008. Induction of autophagy in porcine kidney cells by quantum dots: a common cellular response to nanomaterials? Toxicol. Sci. 106, 140–152.

Su, Y.Y., He, Y., Lu, H.T., Sai, L.M., Li, Q.N., Li, W.X., Wang, L.H., Shen, P.P., Huang, Q., Fan, C.H., 2009. The cytotoxicity of cadmium based, aqueous phase – synthesized, quantum dots and its modulation by surface coating. Biomaterials 30, 19–25.

Su, Y.Y., Hu, M., Fan, C.H., He, Y., Li, Q.N., Li, W.X., Wang, L.H., Shen, P.P., Huang, Q., 2010. The cytotoxicity of CdTe quantum dots and the relative contributions from released cadmium ions and nanoparticle properties. Biomaterials 31, 4829–4834.

Tada, H., Higuchi, H., Wanatabe, T.M., Ohuchi, N., 2007. In vivo real-time tracking of single quantum dots conjugated with monoclonal anti-HER2 antibody in tumors of mice. Cancer Res. 67, 1138–1144.

Tanaka, T., Miyata, T., Inagi, R., Kurokawa, K., Adler, S., Fujita, T., Nangaku, M., 2003. Hypoxia-induced apoptosis in cultured glomerular endothelial cells: involvement of mitochondrial pathways. Kidney Int. 64, 2020–2032.

Tang, M.L., Xing, T.R., Zeng, J., Wang, H.L., Li, C.C., Yin, S.T., Yan, D., Deng, H.M., Liu, J., Wang, M., Chen, J.T., Ruan, D.Y., 2008. Unmodified CdSe quantum dots induce elevation of cytoplasmic calcium levels and impairment of functional properties of sodium channels in rat primary cultured hippocampal neurons. Environ. Health Persp. 116, 915–922.

Vindis, C., Elbaz, M., Escargueil-Blanc, I., Auge, N., Heniquez, A., Thiers, J.C., Negre-Salvayre, A., Salvayre, R., 2005. Two distinct calcium-dependent mitochondrial pathways are involved in oxidized LDL-induced apoptosis. Arterioscler. Thromb. Vasc. Biol. 25, 639–645.

Wu, C.H., Shi, L.X., Li, Q.N., Jiang, H., Selke, M., Ba, L., Wang, X.M., 2010. Probing the dynamic effect of Cys–CdTe quantum dots toward cancer cells in vitro. Chem. Res. Toxicol. 23, 82–88.

Yamawaki, H., Iwai, N., 2006. Cytotoxicity of water-soluble fullerene in vascular endothelial cells. Am. J. Physiol.: Cell Ph. 290, C1495–C1502.

Yu, W.W., Qu, L.H., Guo, W.Z., Peng, X.G., 2003. Experimental determination of the extinction coefficient of CdTe, CdSe, and CdS nanocrystals. Chem. Mater. 15, 2854–2860.